Modeling of Drill String Torsional Vibrations Taking into Account Finite Deformations

L. A. KHAJIYEVA[1], M. M. JANTASSOVA[1], A. K. KUDAIBERGENOV[1, 2,*]
[1]Department of Mathematical and Computer Modelling,
Al-Farabi Kazakh National University,
71 al-Farabi Ave., Almaty, 050040,
KAZAKHSTAN

[2]School of Applied Mathematics,
Kazakh-British Technical University,
59 Tole bi Str., Almaty, 050000,
KAZAKHSTAN

Abstract: - The paper investigates the nonlinear torsional dynamics of drill strings using mathematical and computational modeling. The study is motivated by the need to improve the reliability and efficiency of drilling processes under conditions when torsional vibrations affect the performance and the safety of drilling systems. A nonlinear mathematical model of the drill string is developed by treating it as a deformable rod with distributed parameters. The governing equations are derived from the Hamilton-Ostrogradsky variational principle under the assumption of finite strains within the framework of nonlinear elasticity. The distributed-parameter problem is reduced to a finite-dimensional system by means of the Bubnov-Galerkin method. Numerical simulations are performed to analyze the dynamic response of the considered systems and to evaluate the influence of geometric, dynamic, and physical parameters on drill string vibrations. The results show the effect of drill string length, angular velocity of the drill string, and material properties on the amplitude, frequency characteristics, modal interaction, and phase-plane structure of the nonlinear torsional response.

Key-Words: - dynamics, torsional vibration, drill string, nonlinearity, mathematical model, phase portrait.

Received: January 6, 2026. Revised: March 13, 2026. Accepted: April 9, 2026. Published: July 13, 2026.

1 Introduction

In the oil and gas industry, the drilling process occupies a central position, and its overall efficiency and safety are strongly influenced by the dynamic behavior of the drill string. During rotary drilling, the drill string operates as a long, slender, deformable system that transmits torque and axial load from the surface to the bottom-hole assembly. The efficiency and safety of the drilling process are strongly affected by its dynamic behavior, especially by unwanted vibrations. Among various types of drill string vibrations, torsional vibrations and stick-slip oscillations are of particular concern, since they can cause large oscillations of bit angular velocity, induce severe dynamic loads, accelerate wear of downhole tools, and significantly reduce the rate of penetration, [1], [2]. As modern wells become deeper, more deviated, and more complex, and as drilling systems operate closer to their performance limits, the accurate description and control of drill string torsional dynamics become increasingly important for both design and real-time operations, [1], [3], [4].

In practice, one of the simplest strategies to reduce vibration severity is the proper selection of operating parameters such as rotational speed and weight on bit, often combined with adjustments in drilling fluid properties. These measures can frequently be implemented without hardware modification and may mitigate some harmful regimes. However, the drilling process involves strong nonlinearities and complex couplings between axial, torsional, and lateral motions, as well as interactions with the borehole wall, drilling fluid, and heterogeneous rock formations, [2]. As a result, purely empirical tuning of drilling parameters is not sufficient, and there is a clear need for physically based mathematical and computational models that can capture the essential features of drill string dynamics, including nonlinear torsional behavior and wave propagation along the string, [3], [4], [5].

A wide range of modeling approaches for drill string vibrations has been proposed in the literature. Classical works describe the drill string as a distributed mechanical system and analyze longitudinal and torsional vibrations within a continuum framework, [6]. These models provide a rigorous continuum-mechanics foundation but are mainly developed in linear or weakly nonlinear settings and are often oriented toward analytical analysis rather than comprehensive nonlinear simulations, [7]. More recent studies move towards nonlinear formulations and focus on specific aspects of dynamics. For example, in [4], two lumped-parameter models of different complexity are compared for torsional stick-slip analysis under a unified nonlinear friction law. It is shown that a low-order two-degree-of-freedom model fails to reproduce important features such as bit speed oscillations and nonlinear torque generation, whereas a higher-order model with more degrees of freedom is able to capture wave-like energy transfer and localized torsional oscillations along the drill string.

Finite element formulations are employed in [3], to construct an integrated nonlinear model of the full drill string based on Timoshenko beam theory and a velocity-weakening bit-rock interaction law. This model enables a detailed parametric study of stick-slip vibrations along the drill string and demonstrates that the dominant frequency and amplitude of self-excited torsional vibrations are primarily governed by top drive speed and weight on bit, while the spatial distribution of vibrational energy differs significantly between drill pipes and the bottom-hole assembly. Coupled axial-torsional dynamics are investigated in [2], where a lumped model of the bottom-hole assembly for air drilling is developed. A discrete contact law combined with a rate of penetration model describes the bit-rock interaction. Numerical results show that suitable choices of torsional stiffness, rotary speed, and dynamic loading can suppress both stick-slip and bit-bounce regimes, highlighting the importance of axial-torsional coupling in realistic drilling scenarios.

More complex axial-lateral-torsional behavior is considered in [5], [8]. In [5], an axial-lateral-torsion coupling nonlinear vibration model of a drilling string in curved wells is established using an energy method and Hamiltonian principle. The model accounts for curvature frictional contact with the borehole and the influence of drilling fluid properties. Comparison with field data from several wells confirms its ability to reproduce measured vibration characteristics and stick-slip features. In [8], a four-degree-of-freedom non-smooth model is proposed that couples axial, torsional, and lateral motions, incorporates impacts, friction forces, and torque transmission. The analysis demonstrates how nonsmooth effects and multi-mode coupling can lead to complex dynamic responses, including intermittent contact and large-amplitude vibration bursts.

Beyond individual models, several recent studies provide broader overviews and extensions of drill string dynamics. A comprehensive review of stick-slip vibrations, modeling strategies, and suppression methods is presented in [9], where existing lumped, finite element, and hybrid models are compared, and the main challenges for future work are identified, including the need for better representation of nonlinearities and spatially distributed effects. Lateral-torsional coupling in deviated wells is analyzed in [10], using a nonlinear model based on Lagrange's equations that incorporates drill string-borehole contact, torque dissipation, and borehole trajectory effects. The results show that inclination angle and contact conditions strongly influence lateral displacement and torsional response, especially in highly deviated sections. Distributed-parameter control-oriented models are proposed in [11], where axial-torsional dynamics of a drill string system are described by partial differential equations, and stabilization strategies are developed to attenuate stick-slip oscillations along the entire string. In parallel, experimental and laboratory-scale perspectives are summarized in [12], which reviews design methodologies, experimental configurations, and measurement techniques for drill string vibration tests, emphasizing the importance of realistic scaling, fluid-structure interaction, and integrated multi-mode vibration analysis for validating mathematical models.

Taken together, these works demonstrate a broad spectrum of modeling approaches, ranging from continuum rod theories and finite element formulations to lumped-parameter systems and distributed control models. At the same time, they reveal several important limitations. Continuous models often remain within linear or weakly nonlinear frameworks and are rarely exploited for fully nonlinear torsional regimes. High-fidelity finite element and high-dimensional lumped models provide detailed descriptions but are computationally demanding and less convenient for systematic parametric studies or integration into optimization and control algorithms. Simplified low-order models are attractive due to their tractability but tend to underestimate wave propagation, energy localization, and the full effect of nonlinearities. Furthermore, in many studies, nonlinearity is introduced primarily through the bit-rock friction law, while the structural nonlinearity of the deformable drill string and a unified energy-based formulation derived from variational principles are not explored in sufficient depth.

These observations point to a research gap. There is a lack of nonlinear torsional vibration models for drill string that are systematically derived from a variational framework, explicitly treat the drill string as a deformable system with distributed parameters, incorporate both internal and boundary nonlinearities, and can be reduced in a controlled manner to finite-dimensional systems suitable for efficient numerical analysis and parameter studies. Bridging this gap requires a modeling approach that combines the physical rigor of continuum mechanics with the practicality of reduced-order formulations.

In this study, the drill string is considered as a deformable mechanical system, and torsional vibrations are analyzed within a nonlinear continuous framework. In order to isolate the internal nonlinear torsional response associated with finite deformations, damping, external excitation, and bit-rock interaction are not included in the present formulation. The work aims to develop a nonlinear mathematical model of drill string torsional vibrations and to investigate its dynamic behavior through a numerical analysis. To achieve this aim, the following objectives are pursued. First, a torsional drill string model is constructed based on the Hamilton-Ostrogradsky variational principle with boundary conditions representing drilling operations. Second, the Bubnov-Galerkin method is applied to reduce the distributed-parameter model to a finite system of ordinary differential equations in generalized coordinates. Next, one-, two-, and three-mode approximations are formulated, and the effects of modal truncation are analyzed. Numerical simulations of the reduced systems are then performed. Finally, a parametric study is carried out to evaluate the influence of geometric, dynamic, and physical parameters on torsional vibrations, including their effect on modal interaction and characteristic dynamic responses.

The novelty of this study lies in the development of a variationally consistent nonlinear torsional vibration model with distributed parameters, in which the equations of motion are derived from an energy-based formulation accounting for finite deformations. The proposed approach combines the physical rigor of a continuous model with the computational efficiency of Bubnov-Galerkin reduction and allows one-, two-, and three-mode approximations to be formulated within a unified framework. This makes it possible to analyze the effect of modal truncation, nonlinear modal interaction, and the influence of geometric, dynamic, and material parameters on the local torsional response and phase-plane structure of the drill string.

2 Development of the Mathematical Model

In this section, a nonlinear mathematical model is developed for the torsional vibrations of a drill string treated as an elastic rod. The model is constructed based on the theory of elastic deformation of rod systems developed by [13], under the assumption of finite strains in accordance with the nonlinear elasticity framework of [14], [15]. Such an approach makes it possible to account for geometrically nonlinear effects arising in the deformation of a rotating drill string and to derive the governing equation in a variationally consistent form.

The drill string is considered a slender, deformable structural element transmitting torque to the bottom-hole assembly. Since this study aims to investigate the isolated influence of nonlinear torsional deformation on the dynamics of the drill string, the axial and bending components of motion are neglected in the present formulation. This assumption does not imply that axial and bending vibrations are absent in real drilling systems; rather, it is introduced as a controlled modeling simplification that makes it possible to analyze the torsional mechanism separately while preserving the distributed nature of the model. Such a separation is justified for slender drill strings operating predominantly under rotational loading conditions, where torque transmission and the propagation of torsional waves represent the primary dynamic effects of interest, [6], [11]. The considered formulation is therefore focused on the torsional subsystem, which can be interpreted as a simplified model within a more general coupled nonlinear framework.

Following the rod theory of [13], the displacement field of an arbitrary point of the cross-section is represented in terms of the generalized displacements of the rod axis and the twist angle $\theta(z,t)$. Neglecting transverse shear deformation, the kinematic relations are written as:

$$\begin{aligned} U(x,y,z,t) &= u_1(z,t) + \theta(z,t)y \\ V(x,y,z,t) &= v_1(z,t) - \theta(z,t)x \\ W(x,y,z,t) &= w(z,t) - \frac{\partial u_1(z,t)}{\partial z}x - \frac{\partial v_1(z,t)}{\partial z}y. \end{aligned} \tag{1}$$

where $u_1(z,t)$ and $v_1(z,t)$ are the displacements of the bending center of the cross-section along the x-

and y- axes due to bending, respectively; $w(z,t)$ is the axial displacement along the z-axis; and $\theta(z,t)$. is the angle of rotation of the cross-section relative to the bending center under torsion.

Within the finite-strain formulation of [14], [15], the components of the strain tensor are expressed in terms of relative elongations, shear strains, and rotation angles of the material fiber, which makes it possible to account for geometric nonlinearity caused by finite rotations of the cross-sections of the rod. As noted in [16], removing the restrictions on the magnitude of deformations allows for a more accurate description of the dynamic process and reveals qualitative changes in the vibration behavior.

For the case of pure torsion, the displacement field of the cross-section points (1) is taken in the following form:

$$U(x,y,z,t)=\theta(z,t)y$$
$$V(x,y,z,t)=-\theta(z,t)x \qquad (2)$$
$$W(x,y,z,t)=0.$$

The relative elongations, shear strains, and rotation angles are defined by the following expressions:

$$\begin{gathered} e_{xx}=\frac{\partial U}{\partial x},\ e_{yy}=\frac{\partial V}{\partial y},\ e_{zz}=\frac{\partial W}{\partial z}, \\ e_{xy}=\frac{\partial U}{\partial y}+\frac{\partial V}{\partial x},\ e_{xz}=\frac{\partial U}{\partial z}+\frac{\partial W}{\partial x}, \\ e_{yz}=\frac{\partial V}{\partial z}+\frac{\partial W}{\partial y},\ \omega_x=\frac{1}{2}\left(\frac{\partial W}{\partial y}-\frac{\partial V}{\partial z}\right), \\ \omega_y=\frac{1}{2}\left(\frac{\partial U}{\partial z}-\frac{\partial W}{\partial x}\right),\ \omega_z=\frac{1}{2}\left(\frac{\partial V}{\partial x}-\frac{\partial U}{\partial y}\right), \end{gathered} \qquad (3)$$

where e_{ij} are the components of the tensor of relative elongations and shear strains; ω_i are the rotation angles of an elementary volume relative to x, y, z.

Substituting the field displacement (2) into (3), expression (3) is reduced to the following form:

$$\begin{gathered} e_{xx}=e_{yy}=e_{zz}=e_{xy}=0, \\ e_{xz}=y\frac{\partial\theta}{\partial z},\ e_{yz}=-x\frac{\partial\theta}{\partial z}, \\ \omega_x=\frac{x}{2}\frac{\partial\theta}{\partial z},\ \omega_y=\frac{y}{2}\frac{\partial\theta}{\partial z},\ \omega_z=-\theta. \end{gathered} \qquad (4)$$

The obtained quantities are then used in the formulation of the finite-deformation relations of [14]. As a result, for the considered case (2), the components of the strain tensor take the following form:

$$\begin{gathered} \varepsilon_{xx}=e_{xx}+\frac{1}{2}\left(\omega_y^2+\omega_z^2\right)=\frac{1}{2}\left(\frac{y^2}{4}\left(\frac{\partial\theta}{\partial z}\right)^2+\theta^2\right), \\ \varepsilon_{yy}=e_{yy}+\frac{1}{2}\left(\omega_x^2+\omega_z^2\right)=\frac{1}{2}\left(\frac{x^2}{4}\left(\frac{\partial\theta}{\partial z}\right)^2+\theta^2\right), \\ \varepsilon_{zz}=e_{zz}+\frac{1}{2}\left(\omega_x^2+\omega_y^2\right)=\frac{1}{8}\left(x^2+y^2\right)\left(\frac{\partial\theta}{\partial z}\right)^2, \\ \varepsilon_{xy}=e_{xy}-\omega_x\cdot\omega_y=-\frac{xy}{4}\left(\frac{\partial\theta}{\partial z}\right)^2, \\ \varepsilon_{yz}=e_{yz}-\omega_y\cdot\omega_z=-x\frac{\partial\theta}{\partial z}+\frac{y}{2}\theta\frac{\partial\theta}{\partial z}, \\ \varepsilon_{zx}=e_{zx}-\omega_z\cdot\omega_x=y\frac{\partial\theta}{\partial z}+\frac{x}{2}\theta\frac{\partial\theta}{\partial z}. \end{gathered} \qquad (5)$$

The material of the rod is assumed to be isotropic and physically linear; therefore, the relationship between stresses and strains is described by the generalized Hooke's law for a three-dimensional stress state, [15]. In this case, the density of the elastic potential energy is expressed in terms of the components of the strain tensor and is defined as follows:

$$\begin{gathered} \Phi=G\Big[\varepsilon_{xx}^2+\varepsilon_{yy}^2+\varepsilon_{zz}^2+\frac{\nu}{1-2\nu}\big(\varepsilon_{xx}+ \\ +\varepsilon_{yy}+\varepsilon_{zz}\big)^2+\ 2(\varepsilon_{xy}^2+\varepsilon_{yz}^2+\varepsilon_{zx}^2)\Big], \end{gathered} \qquad (6)$$

where G is the shear modulus, ν is Poisson's ratio, the appearance of which is associated with the use of three-dimensional generalized Hooke's law.

The total potential energy of the rod is determined by Clapeyron's formula:

$$U_0=\int_V\Phi\ dV=\int_0^l\int_A\Phi\ dA\ dz, \qquad (7)$$

where A is the cross-sectional area, l is the length.

After substituting the components of the strain tensor (5) into expression (6) and integrating over the cross-sectional area, the coordinate factors are transformed into geometric characteristics:

$$\begin{gathered} I_p=\int_A(x^2+y^2)\ dA, \\ I_r=\int_A(x^4+y^4)\ dA, \\ I_{x^2y^2}=\int_A x^2y^2\ dA, \end{gathered} \qquad (8)$$

where I_p is the polar moment of inertia, and I_r, $I_{x^2y^2}$ are geometric characteristics of the cross-section.

As a result, the potential energy of the nonlinear system takes the following form:

$$U_0=\int_0^l\left(\frac{G}{1-2\nu}\left\{\frac{I_r}{32}\left(\frac{\partial\theta}{\partial z}\right)^2+\frac{A\theta^4}{2}\right\}+\frac{G(5-6\nu)}{2(1-2\nu)}\left[\frac{I_{x^2y^2}}{16}\left(\frac{\partial\theta}{\partial z}\right)^4+\frac{I_p\theta^2}{4}\left(\frac{\partial\theta}{\partial z}\right)^2\right]+2GI_p\left(\frac{\partial\theta}{\partial z}\right)^2\right)dz. \quad (9)$$

Since the drill string rotates during drilling, the kinetic energy is constructed from the velocity field of the rotating rod, taking into account both torsional deformation rate and rigid-body rotation with angular velocity ω. After substituting the torsional kinematic relations and integrating over the cross-section, it is written as:

$$T=\frac{\rho}{2}\int_0^l I_x\left(\frac{\partial\theta}{\partial t}\right)^2+I_y\left(\frac{\partial\theta}{\partial t}\right)^2+ +I_p\omega^2+I_p\omega^2\theta^2+2I_p\omega\frac{\partial\theta}{\partial t}\Bigg)dz, \quad (10)$$

where ρ is the material density and I_x, I_y are the axial moments of inertia of the cross-section.

The governing equation is derived from the Ostrogradsky-Hamilton variational principle, [17]:

$$\delta\int_{t_1}^{t_2}(T-U_0)\,dt=0. \quad (11)$$

Substituting (9) and (10) into (11), performing the variation with respect to $\theta(z,t)$ and integrating by parts with respect to time and the longitudinal coordinate z, one obtains the nonlinear partial differential equation of torsional motion:

$$\rho I_p\frac{\partial^2\theta}{\partial t^2}=4GI_p\frac{\partial^2\theta}{\partial z^2}-\frac{2AG}{1-2\nu}\theta^3+\frac{G(5-6\nu)}{4(1-2\nu)}I_p\left[\theta^2\frac{\partial^2\theta}{\partial z^2}+\theta\left(\frac{\partial\theta}{\partial z}\right)^2\right]+\frac{G}{8(1-2\nu)}(I_r-I_{x^2y^2}(5-6\nu))\frac{\partial}{\partial z}\left(\frac{\partial\theta}{\partial z}\right)^3+\rho I_p\omega^2\theta. \quad (12)$$

Equation (12) describes nonlinear torsional vibrations of the rotating drill string with allowance for finite strains. Written in this form, it can be interpreted as a nonlinear wave-type equation. Its terms admit the following mechanical interpretation: the time-derivative terms describe torsional inertia; the linear spatial derivative term represents the classical torsional stiffness; the higher-order terms in θ and their spatial derivatives correspond to geometric nonlinearities; and the terms containing ω characterize rotational effects.

In comparison with classical rod vibration models, [13], [18], the resulting equation contains nonlinear terms associated with both the twist amplitude and its spatial gradient, which reflect the geometrically nonlinear character of the deformation process.

The initial conditions are taken as:

$$\theta(z,0)=0,\ \frac{\partial\theta}{\partial t}(z,0)=C\cos\left(\frac{\pi z}{l}\right), \quad (13)$$

where C is a prescribed initial angular velocity parameter. The boundary conditions correspond to zero torsional moment at both ends of the rod:

$$\frac{\partial\theta}{\partial z}(0,t)=0,\ \frac{\partial\theta}{\partial z}(l,t)=0. \quad (14)$$

For further numerical analysis, the distributed-parameter problem (12)-(14) is reduced to a finite-dimensional system by means of the Bubnov-Galerkin method, [19]. The solution is sought in the form:

$$\theta(z,t)=\sum_{i=1}^n\bar{\theta}_i(t)G_i(z), \quad (15)$$

where $G_i(z)$ are basis functions satisfying the boundary conditions. Retaining only the first mode, the approximation is written as:

$$\theta(z,t)=\bar{\theta}_1(t)\cos\left(\frac{\pi z}{l}\right) \quad (16)$$

Introducing the coefficients:

$$k_1=\rho I_p,\ k_2=4GI_p,\ k_3=\frac{2AG}{1-2\nu},\ k_4=\frac{GI_p(5-6\nu)}{4(1-2\nu)},\ k_5=\frac{G(I_r-I_{x^2y^2}(5-6\nu))}{8(1-2\nu)},\ k_6=\rho I_p\omega^2 \quad (17)$$

the governing equation can be rewritten in compact form:

$$k_1 \frac{\partial^2 \theta}{\partial t^2} = k_2 \frac{\partial^2 \theta}{\partial z^2} - k_3\theta^3 + k_4\left[\theta^2 \frac{\partial^2 \theta}{\partial z^2} + \right. \left. +\theta\left(\frac{\partial \theta}{\partial z}\right)^2\right] + k_5 \frac{\partial}{\partial z}\left(\frac{\partial \theta}{\partial z}\right)^3 + k_6\theta. \qquad (18)$$

Substitution of approximation (16) into (18), followed by Bubnov-Galerkin projection over the rod length, leads to a nonlinear ordinary differential equation for the generalized coordinate $\overline{\theta}_1(t)$:

$$a_1 \frac{\partial^2 \overline{\theta}_1}{\partial t^2} + a_2\overline{\theta}_1 + a_3\overline{\theta}_1^3 = 0, \qquad (19)$$

where

$$a_1 = k_1,\ a_2 = \frac{k_2}{l^2} - k_6, \quad a_3 = \frac{3k_3}{4} + \frac{k_4\pi^2}{2l^2} + \frac{k_5\pi^4}{4l^4}. \qquad (20)$$

The initial conditions for the reduced model follow from (13):

$$\overline{\theta}_1(0) = 0,\ \frac{\partial \overline{\theta}_1}{\partial t}(0) = C_1. \qquad (21)$$

The reduced equation (19) has the structure of a Duffing-type nonlinear oscillator, which is a classical model in nonlinear vibration theory, [20]. The linear term determines the small-amplitude torsional frequency, whereas the cubic nonlinear term originates from finite torsional deformation and produces amplitude-dependent stiffness. Thus, equation (19) connects the distributed nonlinear torsional vibration problem with the classical theory of nonlinear oscillations.

In the present study, we deliberately did not employ nondimensionalization. Although this approach is widely used for general analysis, in our case, it does not provide significant advantages, since the objective of the work is a quantitative study of the amplitudes and regimes of torsional vibrations in physically interpretable quantities. A similar approach was also applied in [16], [21].

Similarly to the derivation of the first mode using the Bubnov-Galerkin method, systems of ordinary differential equations are obtained for the two- and three-mode approximations. These systems are not presented in the paper due to space limitations.

3 Numerical Analysis and Discussion

Numerical simulations were performed in Python to analyze the nonlinear torsional response of the drill string and to evaluate the influence of numerical accuracy, modal truncation, and system parameters. The numerical study was organized in several stages. First, the numerical procedure was verified by comparing the Runge-Kutta method with a finite-difference scheme and by analyzing the sensitivity of the solution to the time step. Then, the one-mode approximation was used as a reference case for comparison with higher-mode Bubnov-Galerkin approximations. After that, the nonlinear response was compared with the corresponding linearized model. The influence of modal truncation was assessed by comparing one-, two-, and three-mode Bubnov-Galerkin approximations. Finally, the effects of geometric, dynamic, and material parameters on the torsional response were investigated.

3.1 Numerical Method, Reference Parameters, and Accuracy Verification

The reduced Bubnov-Galerkin equations were integrated in Python using the Runge-Kutta method. It was used due to its stability for nonlinear oscillatory problems and its suitability for time-step refinement.

The reference parameter set for the baseline simulation is given in Table 1, which corresponds to the aluminum drill string.

Table 1. Parameters of the reference drilling system

System parameter	**Value**
Drill string length, l	100 m
Young's modulus, E	0.7×10^{11} Pa
Drill string density, ρ	$2.7\times10^{3}\ \mathrm{kg/m^2}$
Poisson's ratio, ν	0.34
The outer diameter of the drill string, *D*	0.20 m
The inner diameter of the drill string, *d*	0.12 m
Angular velocity, □	$2\pi\times0.5$ rad/s
Initial condition parameter, □	0.1

Source: created by the authors.

Numerical accuracy was assessed by time-step refinement and comparison with a finite-difference scheme. The finest-step Runge-Kutta solution was used as the reference solution. The maximum amplitude and maximum generalized velocity were taken as accuracy indicators, and the relative amplitude difference was calculated as:

$$\delta_A = \frac{\left|A_h - A_{ref}\right|}{A_{ref}} \times 100\%, \qquad (22)$$

where A_h is the maximum amplitude computed for a given time step, and A_{ref} is the corresponding reference value.

Table 2. Numerical accuracy verification for the reference parameter set

Numerical method	**Δt, s**	**Max. amplitude, rad**	**Difference, %**
Runge-Kutta	1.0×10^{-4}	5.061×10^{-4}	0.000
Finite difference	1.0×10^{-3}	5.086×10^{-4}	0.481
Finite difference	5.0×10^{-4}	5.068×10^{-4}	0.120
Finite difference	2.5×10^{-4}	5.063×10^{-4}	0.030
Finite difference	1.0×10^{-4}	5.062×10^{-4}	0.005

Source: created by the authors.

The finest-step Runge-Kutta solution ($\Delta t = 1.0\times10^{-4}$) was taken as the reference solution and is therefore the only Runge-Kutta result reported in Table 2. Runge-Kutta computations with larger time steps gave practically identical amplitudes and therefore are not shown separately. The finite-difference results show clear convergence to the reference solution: the relative amplitude difference decreases from 0.481% at $\Delta t = 1.0\times10^{-3}$ to 0.005% at $\Delta t = 1.0\times10^{-4}$. This confirms the numerical consistency of the obtained solutions.

3.2 One-mode Nonlinear Torsional Response

The one-mode approximation (19) was first analyzed for the reference parameters listed in Table 1. In this case, the torsional motion is described by the generalized coordinate $\bar{\theta}_1(t)$, and the initial excitation is specified by the initial generalized angular velocity C_1.

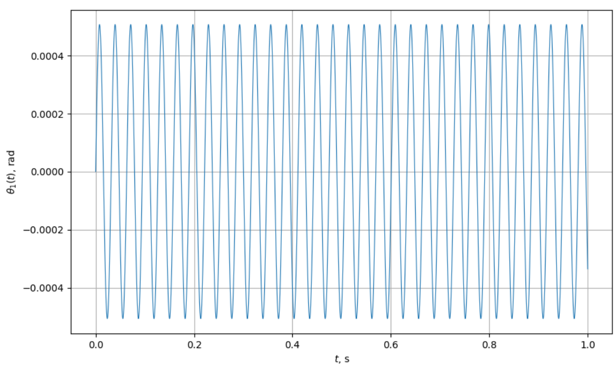

Fig. 1: One-mode nonlinear torsional response for the reference parameter set
Source: created by the authors.

The time history in Figure 1 shows a bounded regular oscillatory response of the one-mode system for $0 \le t \le 1$. For the selected reference parameters and the prescribed initial excitation, the oscillation amplitude remains small. Therefore, the cubic nonlinear term in equation (19) acts mainly as a correction to the dominant linear torsional stiffness and does not lead to a visibly distorted waveform. This is why the response remains close to a harmonic oscillation, although the governing equation contains a nonlinear stiffness term.

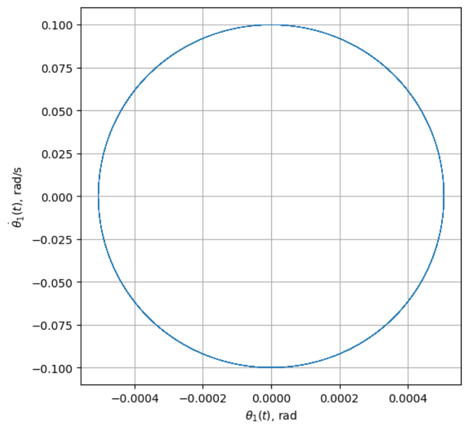

Fig. 2: Phase portrait of the one-mode nonlinear torsional response
Source: created by the authors.

The phase portrait in Figure 2 confirms this behavior. The trajectory remains bounded around the equilibrium point and has a center-type structure.

3.3 Linear and Nonlinear One-Mode Comparison

To evaluate the influence of the cubic stiffness term, the nonlinear one-mode equation was compared with its linearized form obtained by neglecting the term $a_2\theta_1^3$. The comparison was performed for the same reference parameters and initial conditions.

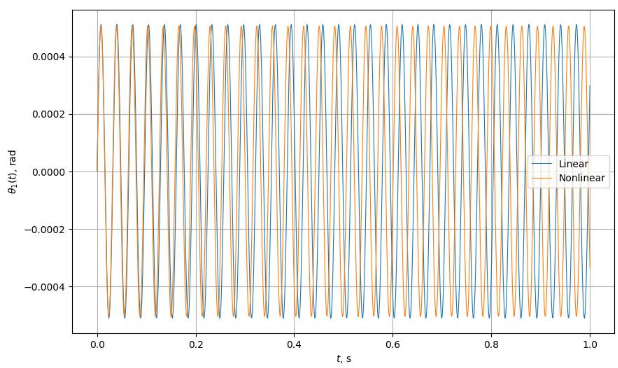

Fig. 3: Linear (blue curve) and nonlinear (orange curve) one-mode torsional responses for $0 \le t \le 1$

Source: created by the authors.

Figure 3 shows that both models produce bounded oscillatory responses. The amplitudes of the two solutions remain close, but the nonlinear response gradually develops a phase shift relative to the linearized solution. This indicates that the cubic finite-deformation term does not primarily change the amplitude level for the considered parameters, but modifies the effective oscillation frequency.

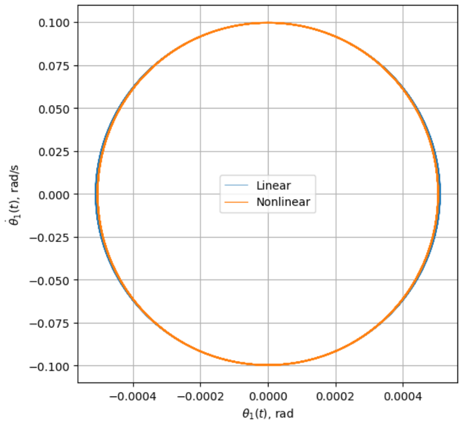

Fig. 4: Phase portraits of the linear (blue curve) and nonlinear (orange curve) one-mode torsional responses
Source: created by the authors.

The phase portraits in Figure 4 confirm that the qualitative stability character is preserved. Both trajectories remain bounded around the equilibrium state and have a center-type structure. Thus, the nonlinear term affects the quantitative characteristics of the response, while the stability type remains unchanged.

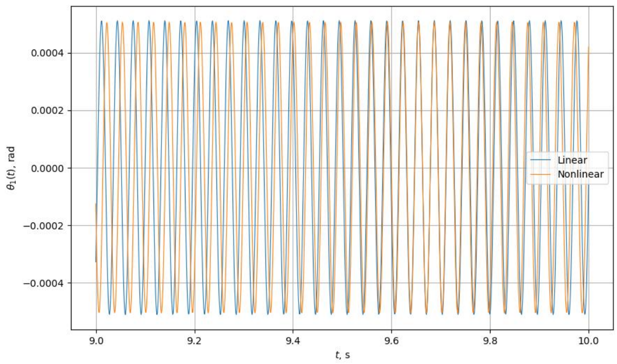

Fig. 5: Linear (blue curve) and nonlinear (orange curve) one-mode torsional responses for $9 \le t \le 10$
Source: created by the authors.

To verify that the phase difference is not limited to the initial part of the simulation, the comparison was also performed on the interval $9 \le t \le 10$. As shown in Figure 5, the linear and nonlinear responses remain bounded, while the accumulated phase shift between the two solutions is still visible. Therefore, in the one-mode approximation, finite-deformation nonlinearity manifests mainly through phase and frequency modification rather than through a qualitative change of the oscillatory regime.

3.4 Analysis of the Two- and Three-Mode Bubnov-Galerkin Approximations

To assess the influence of Bubnov-Galerkin truncation, the numerical analysis was extended from the one-mode approximation (19) to the two- and three-mode models, which were obtained by applying the same Bubnov-Galerkin projection procedure using Python programming language packages.

In contrast to the one-mode case, the multimode approximations include nonlinear coupling terms between the retained generalized coordinates, which allow modal interaction effects to appear in the torsional response.

For the two-mode approximation, the initial modal displacements were taken as zero, while the initial modal velocities were prescribed as:

$$\begin{aligned} &\bar{\theta}_1(0)=0, \ \frac{\partial \bar{\theta}_1}{\partial t}(0)=C_1, \\ &\bar{\theta}_2(0)=0, \ \frac{\partial \bar{\theta}_2}{\partial t}(0)=C_2. \end{aligned} \tag{23}$$

For the three-mode approximation, the initial conditions were extended to:

$$\bar{\theta}_i(0)=0, \ \frac{\partial \bar{\theta}_i}{\partial t}(0)=C_i, \ i=1,2,3. \tag{24}$$

In the computations, the values $C_1=0.1, \ C_2=0.05, \ C_3=0.02$ were used.

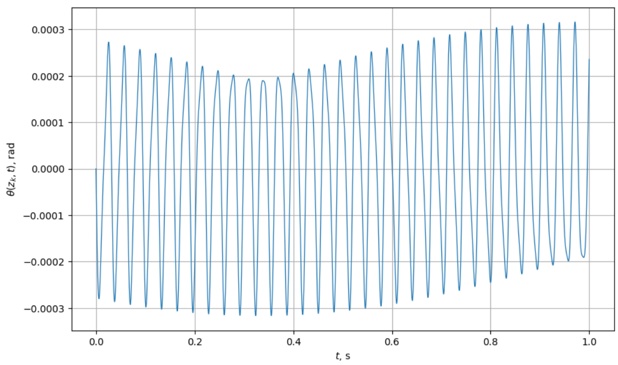

Fig. 6: Two-mode nonlinear torsional responseat the selected sectionfor the reference parameter set in Table 1 z_k
Source: created by the authors.

Figure 6 shows the two-mode torsional response evaluated at the selected section $z_k = 2l/3$. Compared with the one-mode solution, the waveform is no longer purely regular, since the response is formed by the superposition of the first and second modal coordinates. The observed amplitude modulation is caused by nonlinear coupling between these two torsional modes.

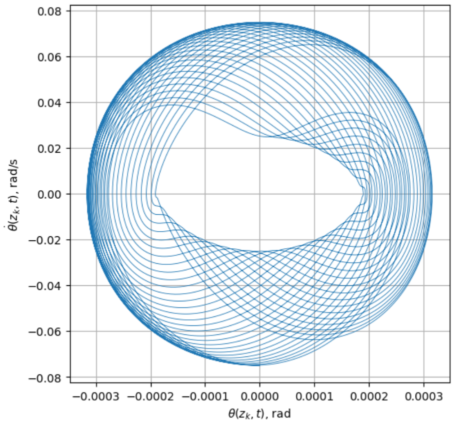

Fig. 7: Phase plane projection of the two-mode nonlinear torsional response
Source: created by the authors.

Figure 7 presents the corresponding phase-plane projection of the two-mode nonlinear torsional vibrations. Unlike the one-mode phase portrait, the projection does not reduce to a simple center-type curve. It remains bounded but occupies a wider and more structured region of the phase plane, reflecting the coupled character of the two-mode system.

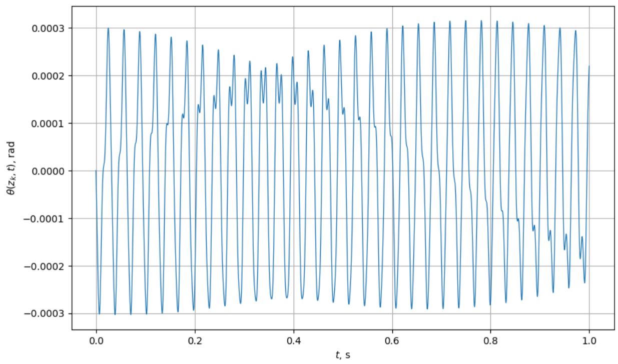

Fig. 8: Three-mode nonlinear torsional response at the selected section for the reference parameter set in Table 1 z_k
Source: created by the authors.

Figure 8 shows the three-mode torsional response at the selected section $z_k = 2l/3$. In this approximation, the local angle of twist is reconstructed from the first three modal coordinates. Compared with the two-mode case, the third mode introduces an additional higher-frequency component into the $\theta(z_k, t)$. As a result, the waveform becomes more modulated, which reflects the combined effect of modal superposition and nonlinear coupling between the retained modes.

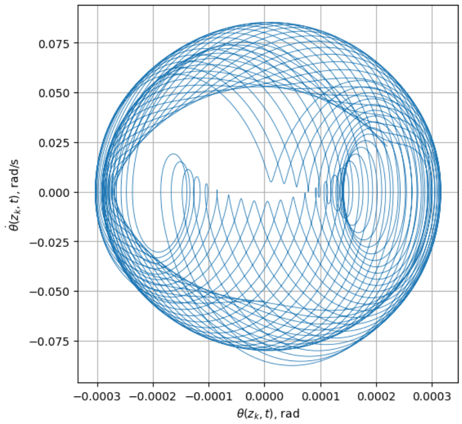

Fig. 9: Phase plane projection of the three-mode nonlinear torsional response
Source: created by the authors.

Figure 9 presents the corresponding phase-plane projectionof the three-mode torsional response. The projection remains bounded, but its structure is more developed than in the two-mode case. This indicates that the third mode affects the detailed form of the torsional response and should be retained when higher-mode interaction is important.

The comparison of one-, two-, and three-mode approximations shows that the one-mode model captures the basic bounded torsional oscillation, whereas the inclusion of higher modes reveals additional modal interaction effects. The two-mode model introduces coupling between the first and second torsional modes, while the three-mode model adds a higher-frequency component and produces a more complex bounded phase-plane projection. Therefore, the multimodal Bubnov-Galerkin approximation provides a more detailed representation of the distributed nonlinear torsional response than the one-mode model.

3.5 Influence of Geometric, Dynamic, and Physical Parameters

After comparing the one-, two-, and three-mode Bubnov-Galerkin approximations, the parametric analysis was performed using the three-mode model. This approximation was chosen because it preserves the dominant torsional mode and includes nonlinear coupling with higher modes.

The same geometric, dynamic, and physical parameters affect all considered modal approximations. However, their influence manifests differently depending on the number of retained modes. In the one-mode model, parameter variation mainly affects the amplitude and frequency of the dominant generalized coordinate. In the three-mode approximation, the same parameters also influence modal interaction, amplitude modulation, and the structure of the phase-plane projection.

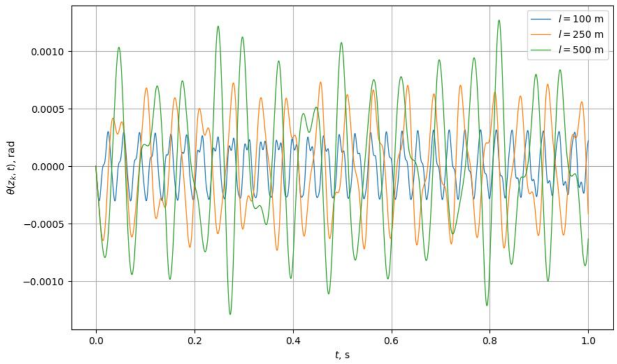

Fig. 10: Three-mode torsional response at the selected section for different drill string lengths: (blue curve), (orange curve), (green curve) $z_k = 2l/3$ $l = 100$ m $l = 250$ m $l = 500$ m

Source: created by the authors.

Figure 10 shows the three-mode torsional response at the selected section z_k for different drill string lengths. The increase in length from $l = 100$ m to $l = 500$ m changes both the amplitude level and the modulation pattern of $\theta(z_k, t)$. For longer drill strings, the reconstructed torsional angle exhibits larger variations, which indicates that the length affects the distribution of the response between the retained modes.

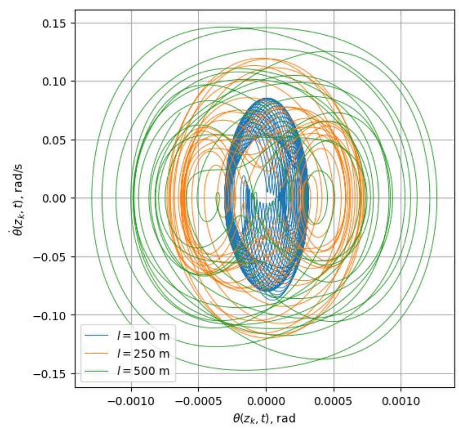

Fig. 11: Phase-plane projections for different drill string lengths: (blue curve), (orange curve), (green curve) $l = 100$ m $l = 250$ m $l = 500$ m

Source: created by the authors.

Figure 11 presents the corresponding phase-plane projections of the three-mode torsional vibrationsfor different drill string lengths. As the length increases, the occupied region in the plane becomes wider and more structured. This shows that the length influences not only the amplitude of the local torsional response, but also the phase evolution and modal interaction pattern. In all considered cases, the projections remain bounded.

Therefore, in the three-mode approximation, the drill string length acts as a significant geometric parameter that modifies both the local torsional amplitude and the structure of the phase-plane response.

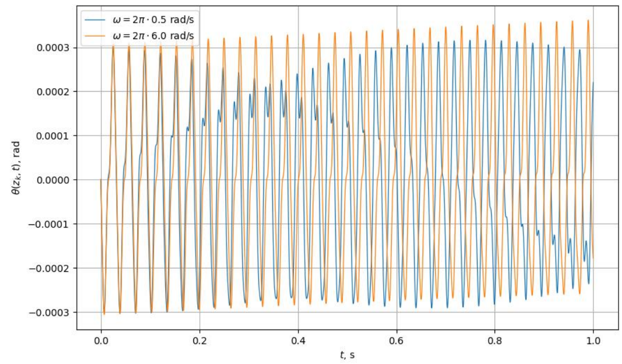

Fig. 12: Three-mode torsional response at the selected section for different angular velocities: (blue curve), (orange curve) $z_k = 2l/3$ $\omega = 2\pi \cdot 0.5$ rad/s $\omega = 2\pi \cdot 6$ rad/s

Source: created by the authors.

Figure 12 presents the three-mode torsional response at the selected section z_k for different angular velocities: $\omega = 2\pi \cdot 0.5$ rad/s and $\omega = 2\pi \cdot 6$ rad/s. It is found that variation in angular velocity changes the modulation structure and the rate of amplitude development, while the system response remains bounded in both cases. This effect is consistent with the reduced equations, where angular velocity enters the effective stiffness through the rotational contribution.

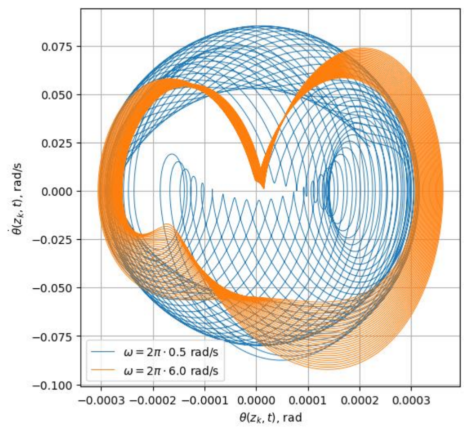

Fig. 13: Phase-plane projections for different angular velocities: (blue curve), (orange curve) $\omega = 2\pi \cdot 0.5$ rad/s $\omega = 2\pi \cdot 6$ rad/s
Source: created by the authors.

The corresponding phase-plane projections are shown in Figure 13. They confirm the bounded character of the motion, but also demonstrate clear differences in the structure of the phase trajectories. This indicates that angular velocity affects not only the time history of the torsional response, but also the phase evolution and modal interaction pattern. Therefore, angular velocity is an important dynamic parameter governing the oscillatory regime of the rotating drill string.

To evaluate the influence of different material properties, the physical parameters for a steel drill string were incorporated into the model, as specified in Table 3.

Table 3. Parameters of the steel drill string used in the comparative analysis

System parameter	**Value**
Young's modulus, E	2.1×10^{11} Pa
Drill string density, ρ	7.8×10^{3} kg / m^2
Poisson's ratio, ν	0.28

Source: created by the authors.

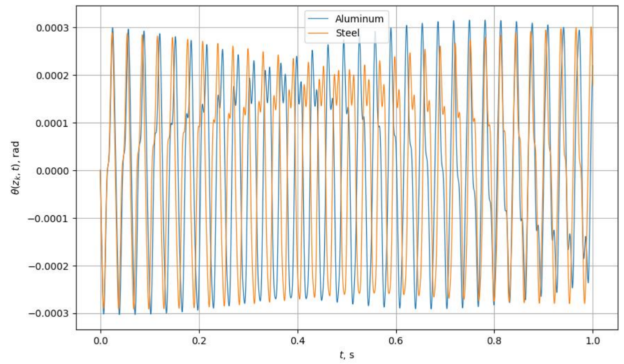

Fig. 14: Three-mode torsional response at the selected section forthealuminum (blue curve) and steel (orange curve) drill string $z_k = 2l/3$
Source: created by the authors.

Figure 14 illustrates the influence of the drill string material on the three-mode torsional response at the selected section z_k. The transition from aluminum to steel changes the elastic and inertial coefficients of the reduced system and leads to a noticeable change in both the amplitude level and the modulation envelope of $\theta(z_k, t)$. Due to the higher stiffness and density of steel, the steel drill string forms a distinct local torsional response, while the motion remains bounded.

The phase-plane projections shown in Figure 15 also differ in their configuration and occupied regions. This indicates that material properties affect not only the amplitude of the torsional response, but also the phase evolution and the interaction between the retained modes. This effect is caused by the combined influence of stiffness and inertia on the dynamics of the multimode system.

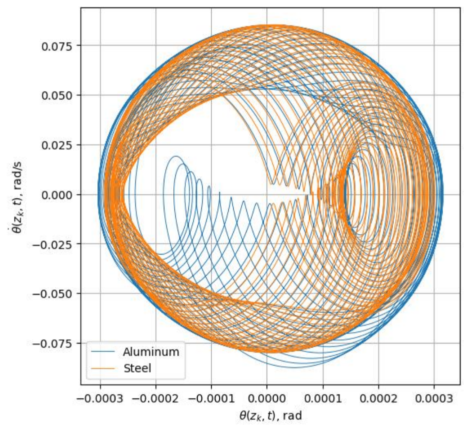

Fig. 15: Phase-plane projections for aluminum (blue curve) and steel (orange curve) drill string
Source: created by the authors.

Thus, material properties have a significant effect on the structure of nonlinear torsional vibrations. In the three-mode approximation, this influence is observed both in the time history and in the phase-plane representation.

3.6 Stability Analysis of the Reduced System

To support the interpretation of the obtained phase portraits and phase-plane projections, the stability properties of the reduced system are analyzed. For the one-mode approximation, the governing equation has the form:

$$a_1 \frac{\partial^2 \bar{\theta}_1}{\partial t^2} + a_2 \bar{\theta}_1 + a_3 \bar{\theta}_1^3 = 0. \tag{25}$$

Introducing the phase variables:

$$x_1 = \bar{\theta}_1,\ x_2 = \frac{\partial \bar{\theta}_1}{\partial t}{}_1, \tag{26}$$

the equation can be rewritten as:

$$\begin{aligned} \dot{x}_1 &= x_2, \\ \dot{x}_2 &= -\frac{a_2}{a_1} x_1 - \frac{a_3}{a_1} x_1^3. \end{aligned} \tag{27}$$

The equilibrium state is $x_1 = 0,\ x_2 = 0.$ Linearization near this equilibrium, giving the Jacobian matrix:

$$J = \begin{pmatrix} 0 & 1 \\ -\dfrac{a_2}{a_1} & 0 \end{pmatrix}. \tag{28}$$

The corresponding characteristic roots are:

$$\lambda_{1,2} = \pm i\sqrt{\frac{a_2}{a_1}}. \tag{29}$$

For the considered parameter values $a_1 > 0,\ a_2 > 0$, therefore, the eigenvalues are purely imaginary. Hence, the equilibrium has a center-type character in the linear approximation. Thus, the one-mode equilibrium is Lyapunov stable, but not asymptotically stable. In the multimodal cases, the plotted curves are phase-plane projections; their bounded form shows that modal coupling changes the trajectory structure without causing instability in the considered parameter range.

4 Conclusion

In this study, a nonlinear mathematical model of drill string torsional vibrations was developed. Based on the Hamilton-Ostrogradsky variational principle and nonlinear elasticity theory with finite strains, the distributed-parameter problem was reduced by the Bubnov-Galerkin method to a finite-dimensional nonlinear ordinary differential equation suitable for numerical analysis.

The numerical results confirmed that the proposed model describes bounded nonlinear torsional oscillations of the drill string and allows the influence of numerical accuracy, modal truncation, and system parameters to be evaluated. Verification by time-step refinement and comparison with a finite-difference scheme demonstrated the consistency of the numerical procedure.

Analysis of the single-mode model confirms the existence of bounded periodic solutions. It was found that the inclusion of cubic nonlinearity mainly renormalizes the effective oscillation frequency and introduces a phase drift without fundamentally altering the stability or amplitude levels typical of the linear regime. However, higher-order approximations like two and three modes capture essential nonlinear phenomena, such as modal energy exchange and complex modulation patterns. The resulting phase-plane projections reflect the increased dimensionality of the system, demonstrating that a multi-mode framework is indispensable for an accurate description of the distributed torsional response.

The parametric analysis based on the three-mode model showed that drill string length, angular velocity, and material properties significantly affect the local torsional response. Increasing the drill string length changes both the amplitude level and the modulation pattern of the torsional angle and leads to wider and more structured phase-plane projections, which are associated with the redistribution of energy between the retained modes and the change in the effective natural frequencies of the system. Variation of angular velocity modifies the modulation structure, phase evolution, and modal interaction pattern due to its contribution to the effective torsional stiffness, while the response remains bounded. The comparison between aluminum and steel drill strings demonstrated that material properties influence both the amplitude envelope and the phase-plane structure as a result of the combined effect of stiffness and inertia. Overall, the results indicate that these parameters govern not only the amplitude of oscillations but also the qualitative features of the nonlinear torsional regime through their influence on modal interaction and energy exchange in the system.

The developed approach is of practical interest for the analysis of drill string dynamics, since it allows one to identify the influence of structural, dynamic, and physical parameters on the torsional response of the system. This creates a basis for a more substantiated selection of operating modes and for improving the reliability and safety of drilling processes.

It should be noted that the present model does not include damping, external excitation, or bit-rock interaction. These effects are not considered to isolate the internal nonlinear torsional dynamics of the drill string within a conservative distributed-parameter formulation. Consequently, the obtained results should be interpreted as describing the internal nonlinear torsional response of the drill string rather than the complete stick-slip drilling process.

Further development of this research will be associated with extending the proposed approach to other deformable mechanical systems, in particular, to the analysis of vibrations of nanobeams and related micro- and nanoscale structures. Special attention may be given to the development of nonlinear models that account for scale-dependent effects, geometric nonlinearity, and complex dynamic interactions in such systems. Another promising direction is the application of the proposed mathematical and computational framework to a wider class of problems in structural mechanics, where nonlinear oscillatory processes play an important role.

References:

[1] Ghasemloonia A., Rideout D.G., Butt S.D., A Review of drillstring vibration modeling and suppression methods, Journal of Petroleum Science and Engineering, Vol. 131, 2015, pp. 150-164. https://doi.org/10.1016/j.petrol.2015.04.030.

[2] Ding S., Fang P., Li G., Lu J., Wang Y., Li Y., Han Y., Xiao D., Axial-torsional nonlinear vibration of bottom hole assembly in the air drilling technology, Petroleum, Vol. 10, No. 3, 2024, pp. 446-461. https://doi.org/10.1016/j.petlm.2023.05.001.

[3] Moharrami M.J., Shiri H., Martins C.A., Numerical Investigation of the Nonlinear Drill String Dynamics Under Stick-Slip Vibration, Vibration, Vol. 7, No. 4, 2024, pp. 1086-1110. https://doi.org/10.3390/vibration7040056.

[4] Doghmane M.Z., Nonlinear Dynamic Modeling and Analysis of Drill Strings Under Stick-Slip Vibrations in Rotary Drilling Systems, Energies, Vol. 18, No. 14, 2025, Art. No. 3860. https://doi.org/10.3390/en18143860.

[5] Liu J., Wang J., Guo X., Dai L., Zhang C., Zhu H., Investigation on axial-lateral-torsion nonlinear coupling vibration model and stick-slip characteristics of drilling string in ultra-HPHT curved wells, Applied Mathematical Modelling, Vol. 107, 2022, pp. 182-206. https://doi.org/10.1016/j.apm.2022.02.033.

[6] Dareing D.W., Livesay B.J., Longitudinal and Angular Drill-String Vibrations with Damping, Journal of Engineering for Industry, Vol. 90, No. 4, 1968, pp. 671-679. https://doi.org/10.1115/1.3604707.

[7] Kamel J.M., Muthalif A.G.A., Falah A.H., A review of vertical drill-string mathematical modeling, Applications in Engineering Science, Vol. 21, 2025, Art. No. 100227. https://doi.org/10.1016/j.apples.2025.100227.

[8] De Moraes L.P.P., Savi M.A., Drill-string vibration analysis considering an axial-torsional-lateral nonsmooth model, Journal of Sound and Vibration, Vol. 438, 2019, pp. 220-237. https://doi.org/10.1016/j.jsv.2018.08.054.

[9] Tang L., Guo B., Zhu X., Shi C., Zhou Y., Stick–slip vibrations in oil well drillstring: A review, Journal of Low Frequency Noise, Vibration and Active Control, Vol. 39, No. 4, 2020, pp. 885-907. https://doi.org/10.1177/1461348419853658.

[10] Tao Z., Meng Y., Feng Q., Yang K., Kang W., Huang X., Fang P., Analysis of nonlinear vibration of lateral-torsional coupling for drill string in deviated well, Journal of Vibroengineering, Vol. 26, No. 7, 2024, pp. 1584–1599. https://doi.org/10.21595/jve.2024.24140.

[11] Tashakori S., Vossoughi G., Zohoor H., van de Wouw N., Prediction-Based Control for Mitigation of Axial–Torsional Vibrations in a Distributed Drill-String System, IEEE Transactions on Control Systems Technology, Vol. 30, No. 1, 2022, pp. 277–293. https://doi.org/10.1109/TCST.2021.3065669.

[12] Maitra E.K., Al Dushaishi M.F., Laboratory-Scale Drillstring Vibration Analysis, Mining, Vol. 5, No. 4, 2025, Art. No. 78. https://doi.org/10.3390/mining5040078.

[13] (text in Russian) Filippov A.P. Vibrations of Deformable Systems, Mashinostroenie, Moscow, 1970. 736 p., ISBN: 978-5-905554-47-6.

[14] Novozhilov V.V., Foundations of the Nonlinear Theory of Elasticity, Dover Publications, New York, 1999, 217 p., ISBN: 978-0486406848.

[15] Lurie A.I., Theory of Elasticity, Springer, Berlin, Heidelberg, 2005, 1050 p., ISBN: 3-540-24556-1. https://doi.org/10.1007/978-3-540-26455-2.

[16] Khajiyeva L., Kydyrbekuly A., Sergaliyev A., Umbetkulova A., Simulation of Movement of Drill Rods at Large Deformations, Advanced Materials Research, Vol. 702, 2013, pp. 253-258. https://doi.org/10.4028/www.scientific.net/AMR.702.253.

[17] Chetaev N.G., Theoretical Mechanics, Springer-Verlag, New York, 1990, 407 p., ISBN: 9780387513799.

[18] Erofeev V.I., Leontieva A.V., Malkhanov A.O., Shekoyan A.V., Nonlinear Longitudinal Magnetoelastic Waves in a Rod with Account of Damage in its Material, Materials Physics and Mechanics, Vol. 35, 2018, pp. 44-52. https://doi.org/10.18720/MPM.3512018_6.

[19] Alyousef H.A., Salas A.H., Alharthi M.R., El-Tantawy S.A., Galerkin Method, Ansatz Method, and He's Frequency Formulation for Modeling the Forced Damped Parametric Driven Pendulum Oscillators, Journal of Low Frequency Noise Vibration and Active Control, Vol. 41, No. 4, 2022, pp. 1426-1445. https://doi.org/10.1177/14613484221101235.

[20] Kovacic I., Brennan M.J. (Eds.), The Duffing Equation: Nonlinear Oscillators and their behavior, John Wiley & Sons, Chichester, 2011, 390 p., ISBN 978-0-470-71549-9. https://doi.org/10.1002/9780470977859.

[21] Kudaibergenov Askar K., Kudaibergenov Askat K., Khajiyeva L.A, On Nonlinear Spatial Vibrations of Rotating Drill Strings under the Effect of a Fluid Flow, WSEAS Transactions on Applied and Theoretical Mechanics, Vol. 18, 2023, pp. 75-83. https://doi.org/10.37394/232011.2023.18.8.

Contribution of Individual Authors to the Creation of a Scientific Article (Ghostwriting Policy)

- L.A. Khajiyeva formulated the research concept, developed the methodological framework of the study.
- M.M. Jantassova developed the nonlinear model, implemented the Bubnov-Galerkin reduction with one-, two-, and three-mode approximations, and carried out the numerical simulations and parametric analysis.
- A.K. Kudaibergenov contributed to the analysis and interpretation of the multimode nonlinear dynamics, including modal interaction effects and phase-plane behavior of the drill string system.

All the authors participated in the preparation of the article.

Sources of Funding for Research Presented in a Scientific Article or Scientific Article Itself

This research is funded by the Science Committee of the Ministry of Science and Higher Education of the Republic of Kazakhstan (Grant No. AP23490543).

Conflict of Interest

The authors have no conflicts of interest to declare that are relevant to the content of this article.